TWO DISTANT EMBEDDED CLUSTERS IN THE OUTER GALAXY

CARLOS A. SANTOS,[1] JOÃO L. YUN,[1] DAN P. CLEMENS,[2] AND RUI J. AGOSTINHO[1]

ABSTRACT

We report the discovery of two distant embedded young stellar clusters located far in the outer Galaxy. The clusters are resolved in near-infrared images and seen as enhancements in the surface density of IR-excess stars centered close to IRAS 07255−2012. The clusters are embedded in a molecular cloud containing a CS dense core. The molecular cloud, as traced by CO ($J = 1$–0) is elongated and extends over a region of 15×6 pc^2. From the millimeter observations, we derive a kinematic distance of 10.2 kpc and a Galactocentric distance of 16.5 kpc, making these clusters among the most distant embedded clusters in the Galaxy. The main (richer) cluster is well confined to a region of about 1.2 pc in radius. Down to our detection limit of about 1–2 $M_\odot$ at this distance, it contains at least 30 members. The smaller cluster contains at least five stars. They all exhibit near-infrared color excesses consistent with young stellar objects having circumstellar and/or envelope material. We estimate that the star formation efficiency of this molecular cloud is about 4%–10%.

Subject headings: ISM: clouds — open clusters and associations: general — stars: formation —
stars: individual (IRAS 07255−2012) — stars: pre–main-sequence

1. INTRODUCTION

Molecular gas in our Galaxy tends to be concentrated toward the lower Galactic latitudes, following mostly the Galactic disk. In addition, molecular gas is most abundant toward the inner Galaxy (e.g., Clemens, Sanders, & Scoville 1988). Since stars form in the cold molecular component of the Galaxy, most star formation has been found and studied in regions of the inner disk and in nearby molecular clouds. Many of these studies have been conducted by near-infrared imaging of known clouds at relatively small distances (e.g., Tapia et al. 1991; Strom, Strom, & Merrill 1993; McCaughrean & Stauffer 1994; Horner, Lada, & Lada 1997; Luhman et al. 1998) and reveal large numbers of young embedded clusters.

A much smaller number of star formation sites are known toward the outer Galaxy and at large Galactocentric distances (>10 kpc). Recently, Kobayashi & Tokunaga (2000) have reported the discovery of seven young stellar objects located in the outer Galaxy at an estimated Galactocentric distance of about 15–19 kpc. However, resolved young embedded clusters located far (e.g., at a heliocentric distance $d > 2.5$ kpc) into the outer Galaxy are virtually unknown, and yet they are important laboratories for understanding star formation and early stellar evolution. Young embedded clusters contain a statistically significant number of stars formed from the same parent cloud. In addition, unlike more evolved open clusters that have lost significant numbers of low-mass stars because of a combination of cluster dynamics and Galactic tides (Vesperini & Heggie 1997), embedded clusters can be used to probe the stellar initial mass function (IMF) down to very low mass stars (e.g., Muench, Lada, & Lada 2000) and its possible variation in space and time.

The small number of known star formation sites located far in the outer Galaxy has made it impossible to perform a systematic analysis of the star formation properties in regions very far from the Galactic center. Different star formation environ-

ments could affect the star formation process, resulting in a different distribution of stellar masses in a cluster (a different IMF) and consequently a different evolution of the stellar components and of the molecular components.

As part of an effort to produce a catalog of protostars and young stellar objects (YSOs) identified in the *IRAS* database, we have discovered two new embedded young stellar clusters located far in the outer Galaxy. The main (richer) cluster is located toward IRAS 07255−2012. In a survey of *IRAS* sources beyond the solar circle, Brand & Wouterloot (1994) obtained a CO map of another *IRAS* source (IRAS 07257−2033) close to IRAS 07255−2012. The size of this map was sufficient to include IRAS 07255−2012, and they report some evidence for outflow activity. Using the 1.2 m southern millimeter-wave telescope at the Cerro Tololo Inter-American Observatory (CTIO) in Chile (with a 8.′8 beam size at 115 GHz), May, Alvarez, & Bronfman (1997) made a CO survey of a large number of molecular clouds in the southern outer Galaxy. They identified a cloud toward IRAS 07255−2012 and derived a distance of 9.3 kpc and a CO mass of $9.5 \times 10^4 \, M_\odot$. In this Letter, we report the discovery of two distant clusters in near-infrared images toward IRAS 07255−2012, characterize their molecular environment, and determine their distance.

2. OBSERVATIONS AND DATA REDUCTION

Millimeter observations were carried out using the Swedish-ESO Submillimeter Telescope (SEST) in Chile during 1999 September and the Five College Radio Astronomy Observatory (FCRAO) telescope in Massachusetts during 2000 April. At SEST, a set of CO ($J = 1$–0) spectra and one CS ($J = 2$–1) spectrum were obtained toward IRAS 07255−2012. We used SIS receivers and the 2000-channel acousto-optical spectrometer as a back end, with a resolution of 43 kHz channel^{-1}. At FCRAO, observations of CO ($J = 1$–0) took place using the 16 pixel SEQUOIA receiver that fed an autocorrelator with 512 channels, resulting in spectra with 0.2 km s^{-1} channels. The CO line appeared relatively narrow, with an FWHM of ∼1.3 km s^{-1}.

Our near-infrared (J, H, and K bands, i.e., $\lambda = 1.25$, 1.65, and 2.2 μm) observations toward IRAS 07255−2012 were con-

[1] Centro de Astronomia e Astrofísica da Universidade de Lisboa, Observatório Astronómico de Lisboa, Tapada da Ajuda, 1349-018 Lisboa, Portugal; csantos@oal.ul.pt, yun@oal.ul.pt, ruiag@oal.ul.pt.

[2] Institute for Astrophysical Research, Boston University, 725 Commonwealth Avenue, Boston, MA 02215; clemens@bu.edu.

ducted during 1999 November using the 1 m YALO[3] telescope at CTIO, which is equipped with the ANDICAM (A Novel Double-Imaging CAMera). The ANDICAM near-infrared array contains 1024×1024 pixels and was used at a plate scale of $0''21$ pixel^{-1}, resulting in a field of view of 3.6×3.6 arcmin^2 on the sky. We obtained two sets of seven dithered frames (of $30''$ step size and following a predefined starlike pattern of the ANDICAM). Due to some vignetting in the camera, the total useful area covered was about 4.5×2.9 arcmin^2 centered $8''$ west and $10''$ south of IRAS 07255−2012. Standard procedures for near-infrared image reduction were applied (e.g., Yun & Clemens 1994), resulting in a final mosaic image for each band. Source extraction and point-spread function photometry were performed on each image using IRAF packages. We found 249 stars present in all J-, H-, and K-band images. We estimate the completeness limit of our images at magnitudes $J = 16.5$, $H = 16$, and $K = 15.5$. Photometry errors range from about 0.08 mag for the bright stars to 0.15 mag for the fainter ones.

3. RESULTS AND DISCUSSION

3.1. *Molecular Material and Distance*

In Figure 1, we present the FCRAO CO ($J = 1$–0) map of velocity-integrated intensity (*contour lines*) toward IRAS 07255−2012 superposed on the optical image from the Digitized Sky Survey (*gray scale*). The strongest emission is seen close to the position of the *IRAS* Point Source Catalog object, coincident with the embedded cluster. To the half-intensity contour, the CO map extends about $5'$ (15 pc) along a direction close to the north-south direction and about $2'$ (6 pc) along the east-west direction. The geometric mean is about 10 pc, which is quite common in the spectrum of Galactic cloud sizes (Terebey, Fich, & Blitz 1986). Using this CO map and standard conversions of integrated CO intensity to H$_2$ column density, we estimate a lower limit for the mass of the cloud of 3.5×10^3 $M_\odot$, in good agreement with estimates of May et al. (1997). This value compares well with a virial mass of about 10^3 $M_\odot$, indicating that the cloud is virialized and bound.

The inset in Figure 1 presents the SEST CS ($J = 2$–1) spectrum obtained toward IRAS 07255−2012. The line is relatively strong (Launhardt et al. 1998), confirming the association with a dense molecular core. The molecular gas displays an LSR velocity of 81.5 km s^{-1}. Assuming a Galactic rotation curve that is essentially flat beyond the solar circle (Clemens 1985) and a Galactocentric distance to the Sun of 8.5 kpc, we derive a kinematic distance of 10.2 kpc to this molecular cloud. This implies a Galactocentric distance of 16.5 kpc. We estimate a distance uncertainty of up to 20% that is due to uncertainties in the rotation curve and to possible streaming motions. Interestingly, at a Galactocentric distance of 16.5 kpc and with Galactic coordinates of $(235°, -1°5)$, this molecular cloud is located within the warp of the outer molecular disk (about 400 pc below the Galactic plane).

Analysis of the Digitized Palomar Sky Survey (DPOSS) optical image of the region toward IRAS 07255−2012 (Fig. 1) supports our conclusion that this cloud is at a large distance. Despite the presence of the molecular cloud and its dense core, no optical obscuration is seen toward the region of CO emission. This is because at large Galactocentric distances, there are not many detectable background stars left to be obscured by the cloud. The scarcity of detectable background stars means that
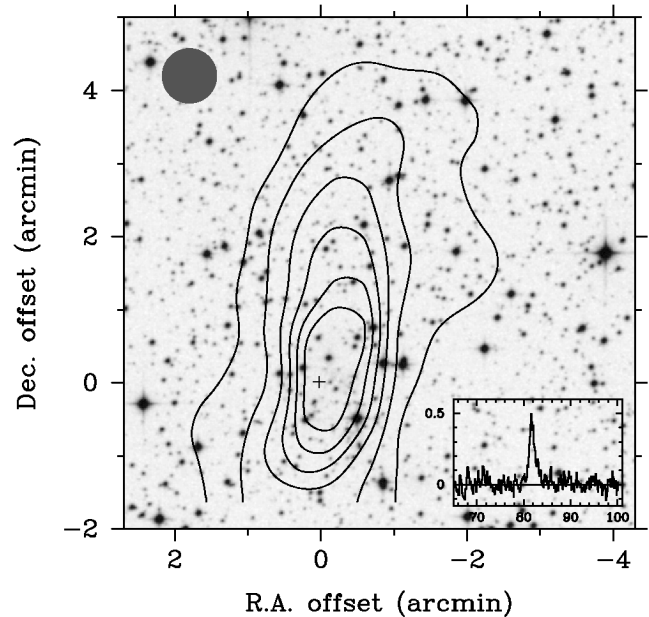
---

[3] Operated by the Yale-AURA-Lisbon-Ohio consortium (Bailyn et al. 1999).

FIG. 1.—Optical image of the region toward IRAS 07255−2012 from the Digitized Sky Survey. The velocity-integrated FCRAO CO ($J = 1$–0) intensity map is superposed on the image. The first contour (4 K km s^{-1}) represents 4 times the noise in integrated intensity. Subsequent contours are at 8, 12, 16, 20, and 24 K km s^{-1}. Notice that despite the presence of the molecular gas as indicated by the CO emission, no obscuration is seen in the optical image. This fact effectively sets a lower limit of about 7 kpc for the distance to this molecular cloud. The inset shows the SEST CS ($J = 2$–1) spectrum toward IRAS 07255−2012 establishing an association with a dense molecular core. The molecular gas displays an LSR velocity of 81.5 km s^{-1}.

the dark cloud does not create any contrast in the surface density of stars between the cloud location and the nearby sky.

To the limiting magnitude of $V = 20$ typical of the DPOSS, we estimate that the obscuration produced by a dark cloud would not be noticeable if the distance to the cloud is larger than about 7 kpc. In order for obscuration to be noticed on optical images, a contrast in the density of background stars between the cloud location (on-cloud) and the nearby sky (off-cloud) must be present on the images. For nearby dark clouds, this contrast is large since most background stars (most dwarfs and giants) can be seen off-cloud. As the distance to the cloud increases, background stars are necessarily more distant. A distance is reached beyond which only O and B main-sequence and giant stars can be detected (to a given detection limit). Because the density of O and B main-sequence and giant stars is small, we take this distance as the limit of detectable obscuration by a dark cloud on optical images. We conclude that the absence of noticeable obscuration produced by this cloud on the DPOSS implies a lower distance limit of about 7 kpc. Virtually all the stars seen in the optical image are foreground stars.

3.2. *Cluster Surface Density and Membership*

Figure 2 presents the YALO H-band image toward IRAS 07255−2012 covering about 4.5×2.9 arcmin^2. The cross indicates the position of the *IRAS* source. In order to identify the presence of clusters and locate their positions, a contour plot of the stellar surface density was made and is shown in Figure 3. The contour levels are set to show significant enhancements (first contour at 3.5 σ) above the average field star den-
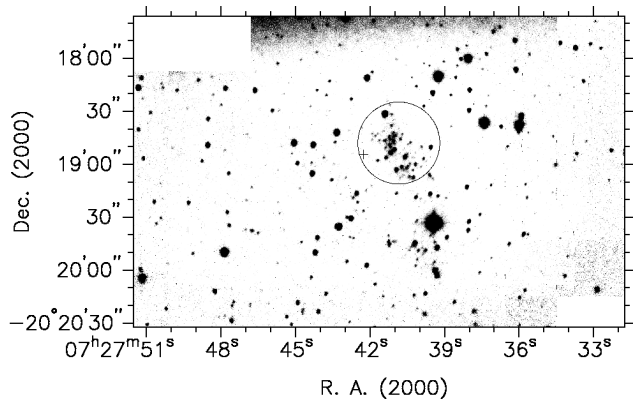
FIG. 2.—*H*-band image toward IRAS 07255−2012 covering about 4.5 × 2.9 arcmin². The new embedded cluster is located inside the circle of 24″ radius, near the center of the image where the stellar density is enhanced. The cross indicates the position of the *IRAS* source.
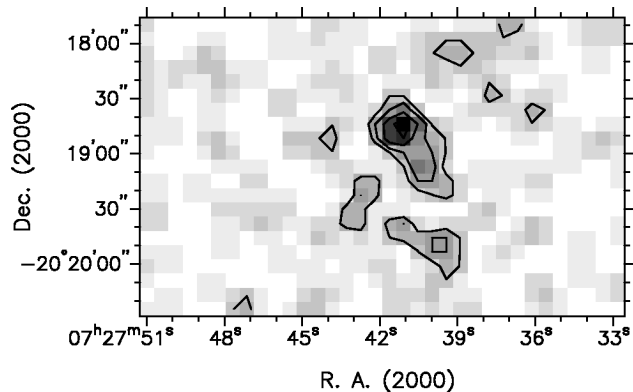

FIG. 3.—Contour plot of the surface density of the cluster. The contour levels are 5.5, 9, 14, and 17.5 stars pc⁻². A main stellar cluster is easily identified and located close to the center. We infer a cluster radius of about 24″. An additional small cluster can be seen about 1′ to the south.

sity. In this figure, we identify a stellar cluster located near the center of the plot. The cluster is circled in Figure 2. The cluster merges with the field for radii beyond about 24″ (1.2 pc), which we take as a lower limit to the cluster radius. Down to the K-band magnitude limit of 16.4, the mean surface density in this cluster (after subtraction of the average field star density of 1.9 pc⁻²) is 6.7 stars pc⁻². Within the 24″ radius, the expected number of cluster members is 30 stars, and the expected number of field stars is nine.

Figures 2 and 3 reveal that about 1′ south of the cluster, there is an additional enhancement of the stellar density. Analysis of the near-infrared colors indicates that five of these stars also have infrared-excess emission. Thus, there is an additional small cluster forming in this molecular cloud about 3 pc to the south of the main cluster. Interestingly, the distribution of molecular material revealed by the CO map is also along a north-south direction and encompasses both clusters.

3.3. *Near-Infrared Photometry and Infrared-excess Emission*

Given the location of this molecular cloud far in the outer Galaxy, we expect that there will be very few detectable background stars. Thus, most or all stars seen toward the cloud should be either foreground or embedded stars. We can use the near-infrared color-color diagram of $(J-H)$ versus $(H-K)$ to distinguish the two cases.

The near-infrared color-color diagram of $(J-H)$ versus $(H-K)$ is shown in Figure 4, where we plot only the stars brighter than $K = 16.4$ in order to avoid large photometry errors. The filled circles represent the objects located within 24″ of the cluster center (inside the circle in Fig. 2). The solid curve is the location of the unreddened main-sequence stars. Two dashed lines parallel to the reddening vector (Koornneef 1983) are superposed. These lines define the reddening band where the main-sequence stars are located if extinguished by dust with standard properties (Rieke & Lebofsky 1985). A large number of sources are located to the right of the reddening band, where objects having infrared-excess emission from circumstellar and/or envelope material are expected to appear (Lada & Adams 1992). Interestingly, for large values of $(H-K)$, most points located to the right of the reddening band correspond to sources contained within the 24″ circle (*filled circles*). This indicates that most cluster members show infrared ex-

cesses similar to YSOs. The points located outside the reddening band and not contained within the 24″ circle (*open circles*) appear either in the small (southern) cluster or within a circle of 1′ radius of the main cluster center. These latter sources could represent a distributed YSO population in the molecular cloud, as is known to exist in nearby molecular clouds (e.g., Lada 1999). Among the filled circles, there is a clear separation between the group of six stars at the lower left-hand corner [those with $(H-K) < 0.6$] and the group of 27 stars at the top right-hand corner of the diagram [those with $(H-K) > 0.6$]. The six stars in the first group can be seen on the DPOSS image and correspond to the foreground main-sequence and giant stars, essentially unreddened. The second group corresponds to stars showing infrared excesses and thus probably are members of the cluster. This is in good agreement with the number of field stars (nine) and of cluster stars (30)
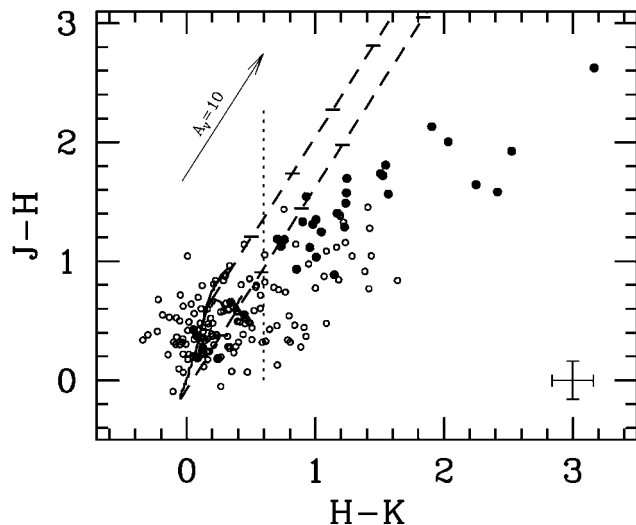

FIG. 4.—Near-infrared color-color diagram of the region toward IRAS 07255−2012 seen in Fig. 2. The filled circles represent the sources contained in a circle of 24″ radius centered at the cluster center (seen in Fig. 2). Most points located to the right of the reddening band are contained within this circle and are likely to be cluster members with infrared-excess emission. The vertical dotted line is located at $(H-K) = 0.6$ and seems to separate the filled circles lying within the reddening band from those lying outside it.

estimated in the previous section. As expected, there is no sign of background-reddened stars in the direction of the cloud, providing additional support to the large distance derived for the cloud and cluster.

At the distance of 10.2 kpc, our limited observations do not detect the low-mass members of this cluster. We estimate the lowest mass star detectable in the cluster by taking the $(J-K)$ color of the faintest member [$m_K = 16.4$, $(J-K) = 1.9$], and we use the color-color diagram to derive $A_V \sim 10$ mag for this source. For an assumed age of about 1 Myr, we estimate that our images are complete down to about 1–2 $M_\odot$ stars. Deeper images are needed to reveal the low-mass stars in this cluster and to determine the location of the expected flattening and turnover of the luminosity function, which is a diagnostic of the age of the cluster (Horner et al. 1997). Thus, we cannot derive accurate constraints on the age of the cluster. However, the large fraction of sources displaying IR excesses suggests that this is a relatively young cluster (less than 1 Myr age) (Strom 1995).

3.4. *Star Formation Efficiency*

The star formation efficiency of this molecular cloud was estimated as follows. First, we assume detection of all young stars down to 1 $M_\odot$. Then, we use a Salpeter IMF down to about 1 $M_\odot$ (with a slope of -1.35) and an essentially flat IMF (with a slope of -0.20) from 1 $M_\odot$ down to the hydrogen-burning limit (Kroupa, Tout, & Gilmore 1993; Leggett, Harris, & Dahn 1994). We use the mass of the molecular cloud derived from CO. The ratio of cluster to cloud masses results in a star formation efficiency of about 4%. This number changes to

about 10% if our images detected stars down to only 2 $M_\odot$. Even though the uncertainty is large, these values are similar to the lower end values of star formation efficiencies found in cluster environments within the local star formation regions (e.g., L1630; Lada 1999).

4. CONCLUSIONS

We have discovered two previously unknown young stellar clusters embedded in a molecular cloud containing a CS dense core. The cloud and clusters are located at a distance of 10.2 kpc and a Galactocentric distance of 16.5 kpc, making these clusters among the most distant young embedded clusters in the Galaxy. The molecular cloud, as traced by CO ($J = 1$–0), is elongated and extends over a region of 15×6 pc^2. It has a mass greater than about 3.5×10^3 $M_\odot$. The main cluster (with at least 30 objects) is detected in our near-infrared images as an enhancement in surface density of IR-excess stars and is confined to a region of about 1.2 pc in radius centered close to IRAS 07255−2012. An additional small cluster (with at least five stars) has also been detected about 3 pc to the south. These findings imply that the physical conditions required for the formation of clusters are met in the very distant environment of the outer Galaxy. We estimate that the star formation efficiency of this molecular cloud is about 4%–10%.

REFERENCES

Bailyn, C. D., DePoy, D., Agostinho, R., Mendez, R., Espinoza, J., & Gonzalez, D. 1999, BAAS, 195, 87.06
Brand, J., & Wouterloot, J. G. A. 1994, A&AS, 103, 503
Clemens, D. P. 1985, ApJ, 295, 422
Clemens, D. P., Sanders, D. B., & Scoville, N. Z. 1988, ApJ, 327, 139
Horner, D. J., Lada, E. A., & Lada, C. J. 1997, AJ, 113, 1788
Kobayashi, N., & Tokunaga, A. T. 2000, ApJ, 532, 423
Koornneef, J. 1983, A&A, 128, 84
Kroupa, P., Tout, C., & Gilmore, G. 1993, MNRAS, 262, 545
Lada, C. J., & Adams, F. C. 1992, ApJ, 393, 278
Lada, E. A. 1999, in The Origin of Star and Planetary Systems, ed. C. Lada & N. Kylafis (Dordrecht: Kluwer), 441
Launhardt, R., Evans, N. J., II, Wang, Y., Clemens, D. P., Henning, T., & Yun, J. L. 1998, ApJS, 119, 59

Legget, S. K., Harris, H. C., & Dahn, C. C. 1994, AJ, 108, 944
Luhman, K. L., Rieke, G. H., Lada, C. J., & Lada, E. A. 1998, ApJ, 508, 347
May, J., Alvarez, H., & Bronfman, L. 1997, A&A, 327, 325
McCaughrean, M. J., & Stauffer, J. R. 1994, AJ, 108, 1382
Muench, A. A., Lada, E. A., & Lada, C. J. 2000, ApJ, 533, 358
Rieke, G. H., & Lebofsky, M. J. 1985, ApJ, 288, 618
Strom, S. E. 1995, Rev. Mexicana Astron. Astrofis. Ser. Conf., 1, 317
Strom, K. M., Strom, S. E., & Merrill, M. 1993, ApJ, 412, 233
Tapia, M., Lopéz, J. A., Rubio, M., Persi, P., & Ferrari-Toniolo, M. 1991, A&A, 242, 388
Terebey, S., Fich, M., & Blitz, L. 1986, ApJ, 308, 357
Vesperini, E., & Heggie, D. C. 1997, MNRAS, 289, 898
Yun, J. L., & Clemens, D. P. 1994, AJ, 108, 612